ACIS CC Mode Observations: New Bias and Split Threshold Parameters and Comparisons to TE data

Nancy Adams-Wolk (SAO) Paul Plucinsky (SAO)

27 October 2003

Abstract

This poster summarizes analyses completed on the Continuous Clocking (CC) mode measurements which used a different bias algorithm for the FI S-array CCDs and also adjusted the split event threshold. A change in the bias algorithm was suggested by Peter Ford to reduce the column-to-column fluctuations in the bias map caused by cosmic ray events which deposit most of their charge along the column direction.

Previous analysis by Ford indicated that the new algorithm reduced these fluctuations but also introduced a small offset to the bias maps. This analysis' primary objective is to relate the performance of the detectors in CC mode to that of TE mode. Specifically, the detection efficiency and gain in CC mode is compared to TE mode.

We first verify the offset in bias maps observed by Ford. We then compare the CC mode measurements with the new bias algorithm and adjusted split threshold with the TE mode based on observations of the external calibration source (ECS). We find that the detection efficiency is not in agreement with the TE mode data, make a correlation between TE and CC calibration products difficult.

Finally, we find that the gain of the CC mode data is significantly different from the TE mode data and we suggest a simple linear correction to the CC mode data which aligns the peaks of the bright lines in the ECS to that in the TE mode data.

Previous work by Divas Sanwal (Chandra Calibration Workshop 2002) also looked for a TE mode to CC mode correlation.

The Observations

Between June 2002 and May 2003, a new bias algorithm was used in the parameter blocks for four ACIS continuous clocking observations of the external calibration source (ECS). All of these observations are on the S-array. Table 3 reports the relevant test parameters.

- OBSIDS 61148 and 61005 are CC mode with current 5-sigma rejection mean bias algorithm.
- OBSIDS 61143 and 60993 are CC mode with 37.5% quartile median bias algorithm.
- OBSIDS 60732 and 60752 are CC mode with 37.5% quartile median bias and a split threshold of 16.
- OBSIDS 61145, 61001 and 60739 are TE mode observations taken in the same weeks as the CC mode observations for comparison.

The default split threshold is 13. The bias algorithm changes were applied to the FI CCDs only. The BI CCDs utilized the 5-sigma rejection mean bias algorithm. Details of the bias algorithms are described in MIT CSR reports from Peter Ford (June 4, 2002 and January 30, 2003).

Data Analysis

This analysis concentrated on four items:

- Total count rate between 0.3-10.0 keV and 0.0-0.3 keV between CC observations with parameter changes and between CC and TE mode observations.
- Rejected/dropped events per frame.
- Confirmation of change of the average bias value with the new bias algorithm.

- Comparison between TE and CC spectra of the ECS to determine differences in gain.

Count Rates

The total count rate between 0.3 and 10.0 keV was examined to determine if there were any obvious changes to the data across the energy range of the ECS emission lines. All of the CC observations used grade_code=10 which will reject ACIS flight grades 24, 66, 107, 214, and 255 on the spacecraft. The data were filtered into a "good" ASCA grade set ([0,2,3,4,6]) and a "bad" ASCA grade set ([1,5,7]). The total number of counts was determined by dmstat. Counts were scaled for the half-life decay of the ECS with respect to OBSID 61148. Exposure times were determined by multiplying the number of non-zero frames by the frame time for that READMODE of ACIS.

Rejected/Dropped Events

Rejected and dropped events reported in the standard data processing (SDP) stat1.fits file were compared to determine if the new parameters caused changes in the event rejections. We examined: DROP_AMP, rejections based on the amplitude of the event; DROP_GRD, rejections based on the grade of the event; and THR_PIX, the number of pixel threshold crossings. An IDL procedure calculated the mean values, the mean errors and the standard deviation for each CCD.

ECS Spectra Comparison

To help define a method to compare the TE mode and the CC mode data, the ECS spectra were examined for both the TE and CC mode data. For the TE mode data, the CXCDS SDP tool acis_process_events was used to apply the CTI corrections to obsids 61001 and 61149. Obsid 60739 was CTI corrected in the SDP and did not go through this step. The centers of the Al-α, Mn-α and Ti-α lines were determined for the TE mode data by using a Gaussian fit to the CTI corrected spectra. Then the CC mode data were also fit to a Gaussian and line centers compared for each of these lines.

Results

Count Rates

Table 1 shows the total count rates over 0.3-10.0 keV.

The change in the CC bias algorithm for obsids 61148 and 60993 caused a decrease in the count rate for both good and bad telemetered ASCA grades in all CCDs, all nodes. The decrease is small, between 0.1-0.4 cts/s. This is expected as the mean bias algorithm tends to overestimate the bias when there are cosmic ray blooms. Correcting for this by using the median bias algorithm should result in a lower overall count rate.

When the CC bias algorithm and the split threshold are changed, the count rate is in agreement with the observations with the mean bias algorithm. This is as expected. The Ford memo 1 discussed how this split threshold change was determined.

The CC mode data is about 1.5 cts/s lower than the TE mode data. This prevents a good correlation between the CC and TE mode count rates.

To compare how the split threshold changes affect the data, we processed observations 60732 and 60752 through acis_process_events with split thresholds between 14-17. At this time, these data are not yet analyzed.

For the bad ASCA grade set, we see a slight increase in count rate across all CC mode observations compared to the TE mode observations. This can also be seen in the spectrum as a small bump at the lower energies. (See Figure 1.) Other than this increase, the low energies show no major discrepancies.

Rejected and Dropped Events

Table 2 displays the average statistics for each type of test. The TE mode data are scaled by 0.5, representing the difference in the defined frame sizes between the modes.

The most interesting result of this analysis was the THR_PIX values. When the bias algorithm is changed to the median, the THR_PIX increases by 300-400 pixels per frame. This is expected as the bias is lower than the mean bias algorithm and more pixels will be above the bias thresholds to be sent to the BEP.

Changing the split threshold and the bias algorithm results in a drop of approximately 250-100 pixels per frame. This is unexpected. The split

threshold change should not affect the number of pixels above the event threshold.

Since the observations with the split threshold occurred 6 months after the previous datasets, we checked the radiation environment to see if a higher radiation background was causing this change. We plotted ACE EPAM P3 level 2 data over the time frames of the observations, but we saw no evidence of a large discrepancy that could change the THR_PIX values.

PH Value in Bias Maps

In repeating the bias analysis that Peter Ford did, the differences between the average bias values were very similar. There was an average change of 2.7 ADU which is only slightly higher than the 2.1 ADU reported in Ford memo 2.

TE vs CC Line Centers

There are two major differences between the TE CTI corrected spectra and the CC mode spectra. The CC mode spectra have broad emission lines, while the CTI corrected TE spectra are narrower and the CC mode spectra are shifted to lower energies with respect to the TE CTI corrected data. The Gaussian fits reveled a shift in PHA could be applied to the CC mode spectra to match the line centers to the TE CTI data. This shift is energy dependent, and can be fit to the function:

shift(PHA) = 11.63 $\pm$ 0.39 + 0.02647 $\pm$ 0.00035 x PHA

This will properly shift the line peaks to align with the CTI corrected TE data. Figure 1 shows the CTI corrected TE data, and the CC mode data with this correction applied. The problem of the CTI in the CC mode remains in the width of the lines. We cannot correct for CTI for these observations of the ECS for CC mode.

References

Ford, Peter, MIT CSR report: ACIS CC-Mode Bias Algorithm, June 4, 2002 *http://acis.mit.edu/acis/ccmode/ccmode1.html (Memo 1)*

Ford, Peter, MIT CSR report: ACIS CC-Mode Bias Algorithm Part 2, January 30, 2003 *http://acis.mit.edu/acis/ccmode/ccmode2.html (Memo 2)*

Acknowledgments

We thank the ACE EPAM instrument team and the ACE Science Center for providing the ACE data.

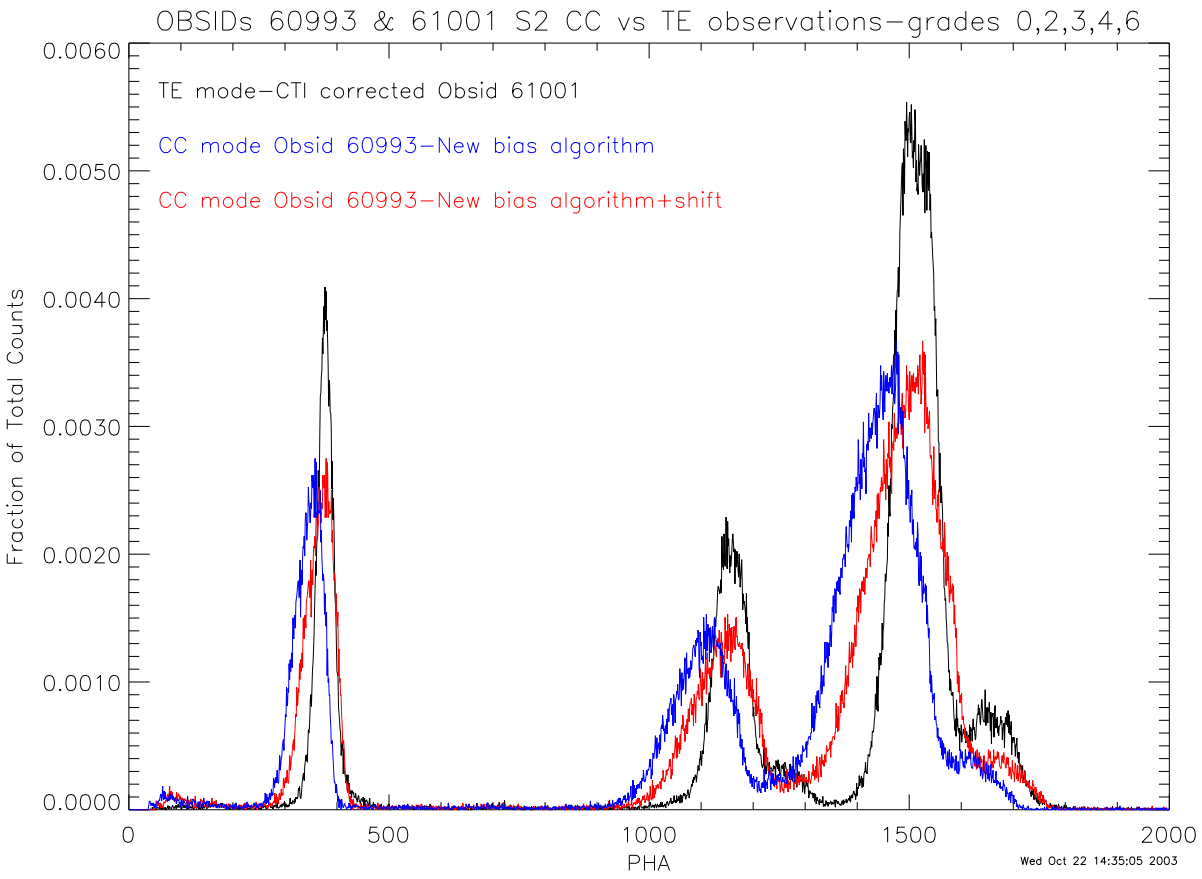

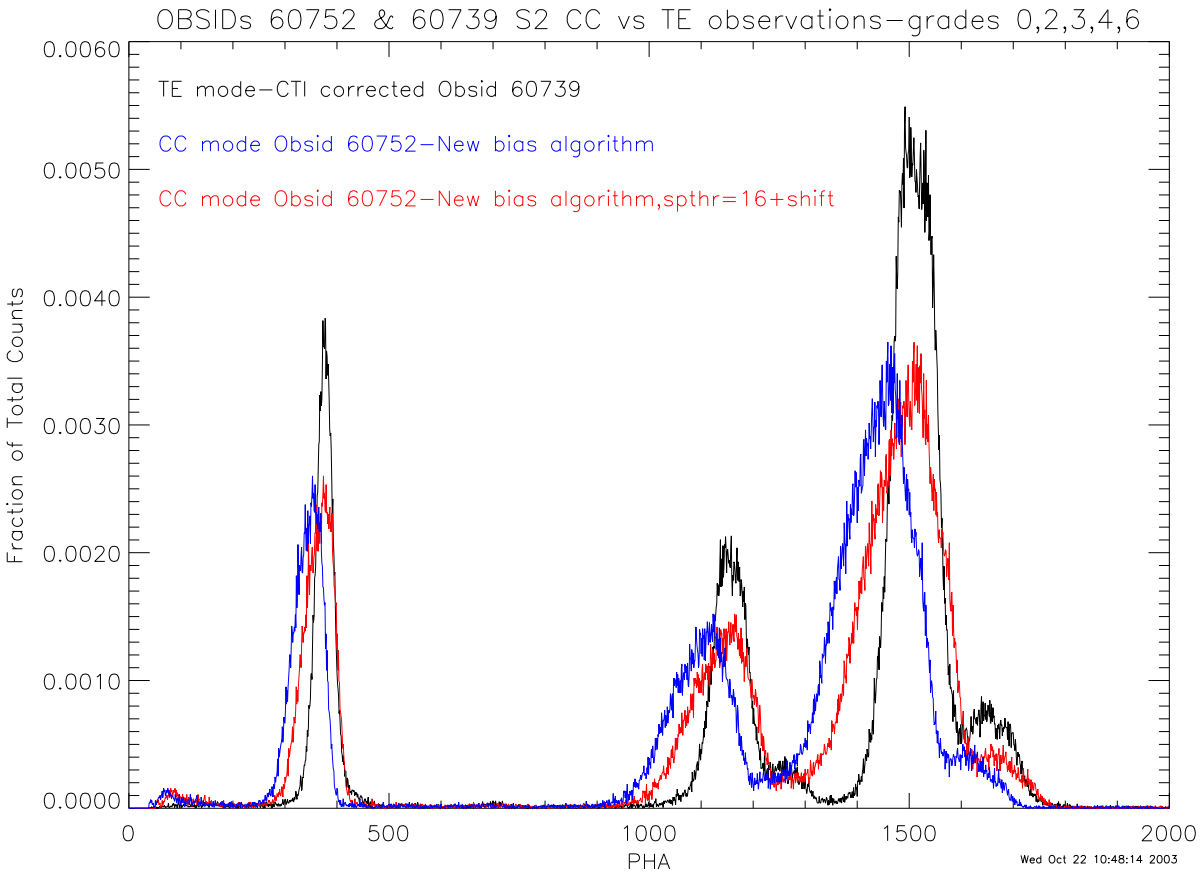

Figure 1: Figure 1: TE CTI corrected data and CC mode data with energy dependent shift applied. Data are for the S2 CCD only. Note that the energy dependent shift holds true for data with spthresh=13 (top panel) and spthresh=16.

CCD 4 Node 0				CCD 4 Node 1			
Grades 0,2,3,4,6		Grades1,5,7		Grades 0,2,3,4,6		Grades1,5,7	
OBSID	Count Rate	OBSID	Count Rate	OBSID	Count Rate	OBSID	Count Rate
61148	10.062± 0.0581	61148	2.388± 0.0283	61148	10.354± 0.0589	61148	2.925± 0.0313
61005	10.203± 0.0600	61005	2.441± 0.0293	61005	10.344± 0.0604	61005	2.998± 0.0325
61143	9.892± 0.0591	61143	2.166± 0.0277	61143	10.247± 0.0602	61143	2.646± 0.0306
60993	10.027± 0.0592	60993	2.382± 0.0288	60993	10.361± 0.0601	60993	2.864± 0.0316
60752	10.062± 0.0520	60752	3.725± 0.0316	60752	10.363± 0.0528	60752	4.377± 0.0343
60732	10.066± 0.0464	60732	4.226± 0.0301	60732	10.373± 0.0471	60732	4.554± 0.0312
60739	11.375± 0.0543	60739	1.973± 0.0226	60739	11.710± 0.0551	60739	2.315± 0.0245
61001	11.351± 0.0623	61001	1.961± 0.0259	61001	11.506± 0.0627	61001	2.272± 0.0279
61145	11.326± 0.0668	61145	1.842± 0.0269	61145	11.559± 0.0674	61145	2.196± 0.0294
CCD 4 Node 2				CCD 4 Node 3			
Grades 0,2,3,4,6		Grades1,5,7		Grades 0,2,3,4,6		Grades1,5,7	
OBSID	Count Rate	OBSID	Count Rate	OBSID	Count Rate	OBSID	Count Rate
61148	10.678± 0.0599	61148	2.850± 0.0309	61148	10.541± 0.0595	61148	2.339± 0.0280
61005	10.569± 0.0611	61005	2.688± 0.0308	61005	10.438± 0.0607	61005	2.128± 0.0274
61143	10.431± 0.0607	61143	2.679± 0.0308	61143	10.418± 0.0607	61143	2.008± 0.0266
60993	10.461± 0.0604	60993	2.746± 0.0310	60993	10.460± 0.0604	60993	2.149± 0.0274
60752	10.610± 0.0534	60752	4.177± 0.0335	60752	10.470± 0.0530	60752	3.381± 0.0301
60732	10.521± 0.0474	60732	4.335± 0.0305	60732	10.591± 0.0476	60732	3.608± 0.0278
60739	11.821± 0.0553	60739	2.228± 0.0240	60739	12.210± 0.0562	60739	1.905± 0.0222
61001	11.741± 0.0633	61001	2.194± 0.0274	61001	11.803± 0.0635	61001	1.744± 0.0244
61145	11.791± 0.0681	61145	2.101± 0.0288	61145	11.829± 0.0682	61145	1.713± 0.0260

CCD 6 Node 0				CCD 6 Node 1			
Grades 0,2,3,4,6		Grades1,5,7		Grades 0,2,3,4,6		Grades1,5,7	
OBSID	Count Rate	OBSID	Count Rate	OBSID	Count Rate	OBSID	Count Rate
61148	11.073± 0.0583	61148	2.029± 0.0250	61148	11.108± 0.0584	61148	2.643± 0.0285
61005	11.010± 0.0588	61005	2.142± 0.0259	61005	11.138± 0.0592	61005	2.604± 0.0286
61143	10.978± 0.0591	61143	2.073± 0.0257	61143	10.978± 0.0591	61143	2.654± 0.0291
60993	10.880± 0.0587	60993	2.024± 0.0253	60993	10.988± 0.0590	60993	2.740± 0.0295
60752	11.141± 0.0523	60752	3.142± 0.0278	60752	11.068± 0.0521	60752	3.842± 0.0307
60732	10.999± 0.0465	60732	3.333± 0.0256	60732	11.191± 0.0469	60732	4.334± 0.0292
60739	12.748± 0.0552	60739	1.573± 0.0194	60739	12.735± 0.0552	60739	2.104± 0.0224
61001	12.561± 0.0625	61001	1.516± 0.0217	61001	12.625± 0.0626	61001	1.894± 0.0243
61145	12.569± 0.0678	61145	1.581± 0.0240	61145	12.665± 0.0680	61145	1.949± 0.0267
CCD 6 Node 2				CCD 6 Node 3			
Grades 0,2,3,4,6		Grades1,5,7		Grades 0,2,3,4,6		Grades1,5,7	
OBSID	Count Rate	OBSID	Count Rate	OBSID	Count Rate	OBSID	Count Rate
61148	11.206± 0.0587	61148	2.438± 0.0274	61148	11.142± 0.0585	61148	2.136± 0.0256
61005	11.284± 0.0595	61005	2.794± 0.0296	61005	11.104± 0.0591	61005	2.209± 0.0263
61143	11.085± 0.0594	61143	2.652± 0.0290	61143	11.053± 0.0593	61143	2.117± 0.0259
60993	11.092± 0.0593	60993	2.759± 0.0296	60993	10.893± 0.0587	60993	2.034± 0.0254
60752	11.127± 0.0523	60752	3.844± 0.0307	60752	11.001± 0.0520	60752	3.380± 0.0288
60732	11.204± 0.0469	60732	4.087± 0.0283	60732	11.064± 0.0466	60732	3.466± 0.0261
60739	12.886± 0.0555	60739	1.968± 0.0217	60739	12.810± 0.0554	60739	1.575± 0.0194
61001	12.681± 0.0628	61001	1.871± 0.0241	61001	12.672± 0.0627	61001	1.893± 0.0243
61145	12.611± 0.0679	61145	1.824± 0.0258	61145	12.659± 0.0680	61145	1.588± 0.0241

CCD 8 Node 0				CCD 8 Node 1			
Grades 0,2,3,4,6		Grades1,5,7		Grades 0,2,3,4,6		Grades1,5,7	
OBSID	Count Rate	OBSID	Count Rate	OBSID	Count Rate	OBSID	Count Rate
61148	11.320± 0.0592	61148	2.466± 0.0276	61148	11.503± 0.0597	61148	2.860± 0.0298
61005	11.359± 0.0590	61005	2.639± 0.0284	61005	11.482± 0.0593	61005	2.992± 0.0303
61143	11.310± 0.0596	61143	2.513± 0.0281	61143	11.307± 0.0596	61143	2.961± 0.0305
60993	11.332± 0.0593	60993	2.712± 0.0290	60993	11.485± 0.0597	60993	2.944± 0.0302
60752	11.435± 0.0524	60752	3.630± 0.0295	60752	11.375± 0.0522	60752	3.871± 0.0305
60732	11.488± 0.0468	60732	4.060± 0.0278	60732	11.517± 0.0468	60732	3.998± 0.0276
60739	12.799± 0.0548	60739	1.731± 0.0202	60739	12.851± 0.0549	60739	1.862± 0.0209
61001	12.879± 0.0619	61001	1.541± 0.0214	61001	12.726± 0.0616	61001	1.742± 0.0228
61145	12.666± 0.0667	61145	1.471± 0.0227	61145	12.684± 0.0668	61145	1.670± 0.0242
CCD 8 Node 2				CCD 8 Node 3			
Grades 0,2,3,4,6		Grades1,5,7		Grades 0,2,3,4,6		Grades1,5,7	
OBSID	Count Rate	OBSID	Count Rate	OBSID	Count Rate	OBSID	Count Rate
61148	11.279± 0.0591	61148	2.750± 0.0292	61148	11.155± 0.0588	61148	2.567± 0.0282
61005	11.450± 0.0593	61005	2.648± 0.0285	61005	11.470± 0.0593	61005	2.724± 0.0289
61143	11.120± 0.0591	61143	2.642± 0.0288	61143	11.103± 0.0590	61143	2.348± 0.0271
60993	11.352± 0.0594	60993	2.991± 0.0305	60993	11.302± 0.0593	60993	2.559± 0.0282
60752	11.326± 0.0521	60752	3.754± 0.0300	60752	11.159± 0.0517	60752	3.694± 0.0298
60732	11.291± 0.0464	60732	3.984± 0.0275	60732	11.382± 0.0465	60732	3.766± 0.0268
60739	12.884± 0.0550	60739	1.912± 0.0212	60739	12.767± 0.0548	60739	1.735± 0.0202
61001	12.857± 0.0619	61001	1.959± 0.0242	61001	12.678± 0.0614	61001	1.666± 0.0223
61145	12.652± 0.0667	61145	1.787± 0.0251	61145	12.678± 0.0667	61145	1.632± 0.0239

CCD 9 Node 0				CCD 9 Node 1			
Grades 0,2,3,4,6		Grades1,5,7		Grades 0,2,3,4,6		Grades1,5,7	
OBSID	Count Rate	OBSID	Count Rate	OBSID	Count Rate	OBSID	Count Rate
61148	10.652± 0.0578	61148	2.262± 0.0266	61148	10.750± 0.0581	61148	2.378± 0.0273
61005	10.846± 0.0585	61005	2.267± 0.0268	61005	10.744± 0.0583	61005	2.771± 0.0296
61143	10.642± 0.0583	61143	2.138± 0.0261	61143	10.540± 0.0580	61143	2.542± 0.0285
60993	10.621± 0.0591	60993	2.135± 0.0265	60993	10.699± 0.0593	60993	2.632± 0.0294
60752	10.770± 0.0517	60752	3.444± 0.0292	60752	10.856± 0.0519	60752	3.692± 0.0303
60732	10.699± 0.0464	60732	3.721± 0.0274	60732	10.855± 0.0467	60732	4.079± 0.0286
60739	12.298± 0.0549	60739	1.760± 0.0208	60739	12.379± 0.0551	60739	1.912± 0.0217
61001	12.116± 0.0619	61001	1.705± 0.0232	61001	12.301± 0.0624	61001	1.923± 0.0247
61145	12.200± 0.0672	61145	1.791± 0.0257	61145	12.273± 0.0674	61145	1.871± 0.0263
CCD 9 Node 2				CCD 9 Node 3			
Grades 0,2,3,4,6		Grades1,5,7		Grades 0,2,3,4,6		Grades1,5,7	
OBSID	Count Rate	OBSID	Count Rate	OBSID	Count Rate	OBSID	Count Rate
61148	10.791± 0.0582	61148	2.896± 0.0301	61148	10.427± 0.0572	61148	1.852± 0.0241
61005	10.828± 0.0585	61005	2.610± 0.0287	61005	10.586± 0.0578	61005	2.023± 0.0253
61143	10.582± 0.0581	61143	2.613± 0.0289	61143	10.323± 0.0574	61143	1.884± 0.0245
60993	10.564± 0.0589	60993	2.646± 0.0295	60993	10.312± 0.0582	60993	1.879± 0.0249
60752	10.643± 0.0514	60752	3.912± 0.0311	60752	10.480± 0.0510	60752	2.804± 0.0264
60732	10.793± 0.0466	60732	4.408± 0.0298	60732	10.452± 0.0459	60732	2.863± 0.0240
60739	12.223± 0.0548	60739	2.102± 0.0227	60739	12.068± 0.0544	60739	1.323± 0.0180
61001	12.104± 0.0619	61001	1.844± 0.0241	61001	12.024± 0.0617	61001	1.290± 0.0202
61145	12.144± 0.0670	61145	1.863± 0.0263	61145	11.969± 0.0665	61145	1.261± 0.0216

Figure 2: Table 1: Count Rates for 0.3-10.0 keV for each CCD/node.

Mean Dropped Data Statistics per FRAME

OBSID	ccd	DROP_AMP	stdev	DROP_GRD	stdev	THR_PIX	stdev
61148&61005	4	61.369± 0.18	23.86	237.256± 0.35	121.61	7698.360± 1.97	3002.59
test averages	6	69.004± 0.18	26.38	188.841± 0.29	97.05	6882.508± 1.77	2595.88
CC mean bias	8	63.751± 0.17	24.37	186.717± 0.29	99.83	6613.560± 1.72	2586.85
	9	65.221± 0.17	24.50	199.610± 0.30	115.74	7066.209± 1.80	2689.88
61143&60093	4	60.537± 0.18	23.37	260.475± 0.37	132.85	8106.044± 2.04	3048.49
test averages	6	68.524± 0.18	25.71	208.857± 0.31	111.15	7295.561± 1.84	2721.26
CC median bias	8	64.123± 0.17	23.94	202.283± 0.30	102.99	6970.528± 1.78	2596.89
	9	64.345± 0.17	24.99	223.780± 0.33	185.45	7485.182± 1.88	2985.24
60732&60752	4	58.239± 0.14	22.92	231.036± 0.28	130.03	7559.510± 1.63	3087.74
test averages	6	66.117± 0.15	24.42	190.208± 0.25	102.57	6899.079± 1.49	2624.47
CC median bias	8	61.398± 0.14	24.36	181.359± 0.24	99.79	6476.017± 1.42	2570.13
spthresh=16	9	62.992± 0.14	24.57	200.283± 0.26	117.12	7011.597± 1.51	2773.45
60738,61001	4	61.391± 0.18	21.40	215.154± 0.34	88.39	6994.357± 1.93	2068.86
&61149	6	68.977± 0.18	22.40	172.837± 0.29	76.90	6391.763± 1.77	1870.72
test averages	8	62.764± 0.17	21.19	166.049± 0.28	73.63	6156.617± 1.71	1868.58
TE mode	9	66.132± 0.18	22.10	184.895± 0.30	77.43	6614.188± 1.82	1943.81

Figure 3: Table 2: Dropped Data Statistics averaged across tests of like parameters.

Test	OBSID	Date	SIMODE	FPBtemp[1]	FPtemp[2]	Description
CC_B1	61148	28, June 2002	CC_0006A	-116.9	-118.0	mean bias, spThresh=13
CC_B2	61143	1, July 2002	CC_0006E	-117.6	-118.8	median bias, spThresh=13
CC_B3	61005	9, Oct 2002	CC_0006A	-119.8	-119.7	mean bias, spThresh=13
CC_B4	60993	17, Oct 2002	CC_0006E	-119.8	-119.8	median bias, spThresh=13
CC_B5	60752	4, May 2003	CC_00080	-119.4	-119.6	median bias, spThresh=16
CC_B6	60732	22, May 2003	CC_00080	-120.0	-119.8	median bias, spThresh=16
	61001	9, Oct 2002	TE_0021C	-119.7	-119.7	TE CTI measurement
	60739	14, May 2003	TE_0021C	-119.9	-119.8	TE CTI measurement
	61145	28, June 2002	TE_0021C	-119.8	-119.8	TE CTI measurement

[1]focal plane temperature during bias

[2]focal plane temperature during event collection

Figure 4: Table 3: Observations used and test parameters.